Supporting Information

Stretchable Supercapacitor at -30 ºC

Xuting Jin,§[a,b] Li Song,§[a], Hongsheng Yang,[c] Chunlong Dai,[a] Yukun Xiao,[a] Xinqun Zhang,[a] Yuyang Han,[a] Congcong Bai,[a] Bing Lu,[a] Qianwen Liu,[a] Yang Zhao,[a] Jiatao Zhang,[a,b] Zhipan Zhang,[a]* Liangti Qu[d]*

[a] Key Laboratory of Photoelectronic/Electrophotonic Conversion Materials, Key Laboratory of Cluster Science, Ministry of Education of China, School of Chemistry and Chemical Engineering, Beijing Institute of Technology, Beijing 100081, P. R. China.

Email: zhipan@bit.edu.cn (Zhipan Zhang)

[b] School of Materials Science and Engineering, Beijing Institute of Technology, Beijing 100081, China.

[c] Laboratory of Rubber-Plastics, Ministry of Education/Shandong Provincial Key Laboratory of Rubber-Plastics, Qingdao University of Science & Technology, Qingdao City 266042, People's Republic of China

[d] Key Lab of Organic Optoelectronics and Molecular Engineering of Ministry of Education, Department of Chemistry, Tsinghua University, Beijing 100084, P. R. China.

Email: lqu@mail.tsinghua.edu.cn (Liangti Qu)

§ These authors contributed equally to this work.

Methods

Synthesis of the anti-freezing organohydrogel polyelectrolyte and the cross-linked polyacrylamide hydrogel polyelectrolyte: First, 6 g of AM (Acros Organics) was dispersed in 20 mL deionized water under the ultrasonic condition and then methylene-bis-acrylamide (0.003 g, Energy Chemical) was added into the solution. Sequentially,

15 μL of N, N, N', N'-tetramethyl-ethylenediamine (TMED) catalysts (Energy Chemical) and 0.02 mg of ammonium persulfate (APS) (Sigma-Aldrich) initiators were added to initiate polymerization under stirring. Then, the mixed solution were quickly poured in plastic vessels. After sealing and then reacting at 50 ºC for 24 h, the cross-linked polyacrylamide hydrogel was obtained. Then, the anti-freezing organohydrogel polyelectrolyte (AF-OHP) were obtained by soaking the dried gels in 10 wt% of sulfuric acid ethylene glycol/water (v:v=1:1) solution for 72 h to achieve the equilibrated state. The cross-linked polyacrylamide hydrogel polyelectrolyte was prepared by soaking the cross-linked polyacrylamide hydrogel in 10 wt% of sulfuric acid aqueous solution for the same time. Similarly, control polyelectrolytes with different proportion of ethylene glycol/water (v/v=0, 1/3, 3/1) are prepared through the aforementioned method similar to AF-OHP to construct control SCs.

Fabrication of the supercapacitors

First, 5 mmol of aniline monomer (Macklin) was added into the 30 mL of above-mentioned sulfuric acid ethylene glycol/water solution with the same the same proportion under stirring in 0 ºC for 10 min. Then, 3.33 mmol of APS was dissolved in 20 mL of the same sulfuric acid ethylene glycol/water solution under stirring and ultrasonic conditions at 0 °C. Next, the crosslinked AF-OHP with different sizes was immersed into sulfuric acid ethylene glycol/water solution containing 5 mmol of aniline monomer for 0.5h. Then, as-prepared APS solution was added to initiate polymerization under stirring for 12 h at the room temperature. Finally, an antifreezed, essentially stretchable and truly integrated SC (AF-SSC) was fabricated by cutting their edges of the obtained sandwich-like block with the deposited PANI onto the two-sided faces to avoid the short circuit. Similarly, the different contrasted SCs (CSC, CSC-1/3 and CSC-3/1) based on the prepared polyelectrolytes with different proportion of ethylene glycol/water (v/v=0, 1/3 and 3/1) were also fabricated through the aforementioned method similar to AF-SSC, respectively. We utilize carbon nanotube paper (Chengdu Organic Chemicals Co. Ltd., Chinese Academy of Sciences, China) as wire to directly fixed on both ends of the device for testing due to the strong stickiness of AF-SSC. Similarity, an integrated SC based on other conductive polymer such as poly (3, 4-

ethylenedioxythiophene) (PEDOT) (Alfa) by using a similar construction strategy.

Characterizations: The morphologies of the samples were observed and investigated by SEM (JSM-7500F). Raman spectra and FT-IR spectra were carried out by a Horiba JY HR-800 Raman spectrometer and a Bruker VERTEX 700 spectrometer, respectively. X-ray diffraction (XRD) were tested by adopting Netherlands 1,710 diffractometer with a Cu-Kα irradiation source (λ=1.54 Å). A material testing system (SHIMADZU AGS-X) and DMA 850 was used to record the mechanical tensile tests. The performance of the device at low temperatures was tested with the aid of a commercial cryogenic refrigerator (Guangzhou Aoxue Refrigeration Equipment Co., Ltd., China). The ionic conductivity of the polyelectrolyte can be calculated by the relationship: $\sigma = L/(RA)$, where L is the height between the current collectors, A is the contact area (m^2) between the polyelectrolyte and the current collectors, and R is the resistance measured by sandwiching the polyelectrolyte between two Au plates as current collectors using a CHI 760E electrochemical workstation. GCD profiles, CV curves, and electrochemical impedance spectroscopy (EIS) measurements of SCs were obtained by using a CHI 760E electrochemical workstation in two electrode configuration. The specific capacitance (C) can be calculated according to the single electrode data following the formulae: $C = I\triangle t/(AU)$, $C=(\int IdV)/(2UvA)$, where $\triangle t$, I, U, $\int IdV$, v, and A is the discharging time, the discharge current, and the voltage variation (excluding the IR drop), the integrated area of the CV curve, scan rate and the area of SC, respectively. The adhesiveness of the SC was characterized by a tensile-adhesion test using different substrate materials on a universal mechanical testing machine (SHIMADZU AGS-X), according to previous literature [1, 2].

Density Functional Theory (DFT) Calculations

The simulation was performed using the density functional theory program $DMol^3$ in Material Studio (Accelrys, San Diego, CA)[1, 3]. The physical wave functions were is extended in terms of numerical basis sets, $Dmol^3$ /GGA-PBE/DNP(3.5) basis set, which is comparable to 6-31G** basis sets. The core electrons are processed by the DFT semi-core pseudo potential. Perdew-Burke-Ernzerhof (PBE) generalized gradient approximation (GGA) is used to calculate exchange correlation energy. A Fermi

smearing of 0.005 Ha (1 Ha = 27.211 eV) and a global orbital cutoff of 5.2 Å were utilized. The convergence criteria for geometric optimization and energy calculation were set as follows: (a) Self-consistent field tolerance was 1.0×10^{-6} Ha/atom; (b) Energy tolerance was 1.0×10^{-5} Ha/atom; (c) The maximum force tolerance was 0.002 Ha/Å; (d) The maximum displacement tolerance was 0.005Å.

Interaction energy calculation

The interaction energy (E_{int}) is obtained according to the following equation, which represents the intensity of the interaction between the various components in the system:

$$\mathbf{E_{int}=E_{total}-\sum E_{component}} \quad (1)$$

where E_{total} and $E_{component}$ represent the total energy of the system, and the energy of each component in the system, respectively. A negative Eads value corresponds to stable adsorption between components. More negative E_{int} represents a stronger interaction in the system.

Reference

[1] F. Mo, G. Liang, Q. Meng, Z. Liu, H. Li, J. Fan and C. Zhi, *Energy Environ. Sci.*, 2019, **12**, 706-715.

[2] L. Han, Y. Zhang, X. Lu, K. Wang, Z. Wang and H. Zhang. *ACS Appl. Mater. Interfaces*, 2016, **8**, 29088-29100.

[3] L. Han, K. Liu, M. Wang, K. Wang, L. Fang, H. Chen, J. Zhou and X. Lu, *Adv. Funct. Mater.*, 2018, **28**, 1704195.

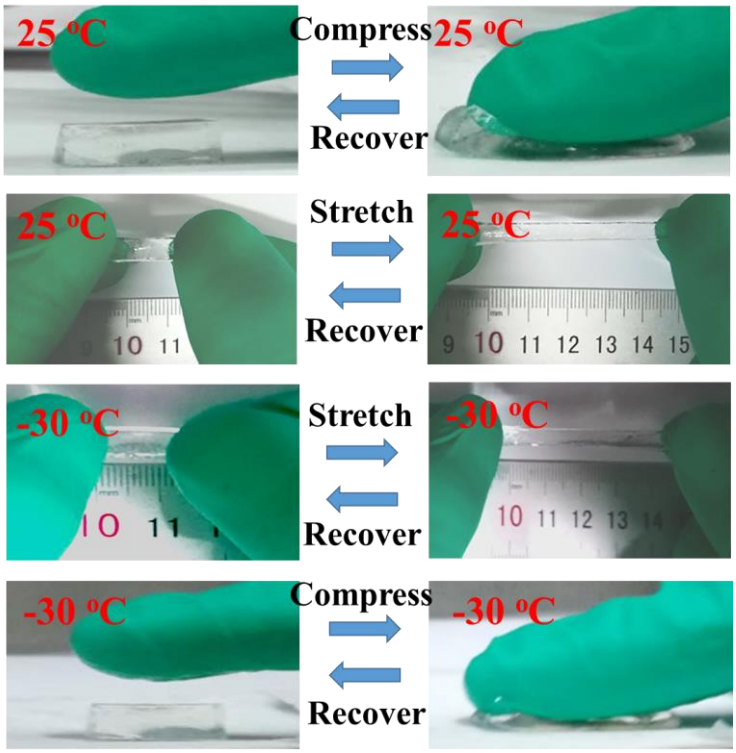

Figure S1. The high compression and excellent stretchability of AF-OHP at 25 ºC and -30 °C.

Figure S2. The minimum thickness (~1.3 mm) of AF-SSC.

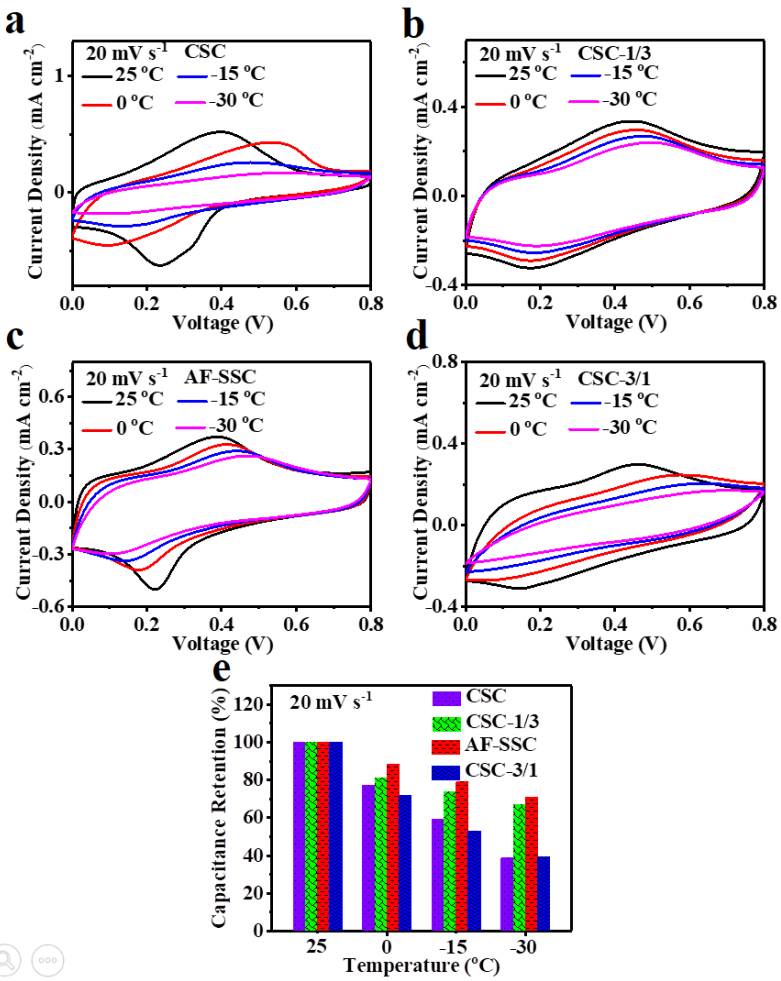

Figure S3. a-d) The CV curves under different temperature of the integrated CSC, CSC-1/3, AF-SSC, CSC-3/1 when the volume ratios of EG/W are 0, 1/3, 1/1, 3/1, respectively. e) The capacitance retention of CSC, CSC-1/3, AF-SSC, and CSC-3/1 under the different temperature. In order to investigate the influence of the addition of EG on the anti-freezing performance, SCs denoted as CSC, CSC-1/3, AF-SSC and CSC-3/1 were fabricated with electrolytes the volume ratios of EG/W are 0, 1/3, 1/1, 3/1, respectively. Obviously, the capacitance retention of AF-SSC under 0 °C, -15 °C and -30 °C at the scan rate of 20 mV s^{-1}, reach 88.3%, 79% and 71%, respectively, preceding those of other three control SCs (Fig. 6d and Supplementary 15).

Figure S4. The integrated device units of different shapes prepared by simple cutting technology.

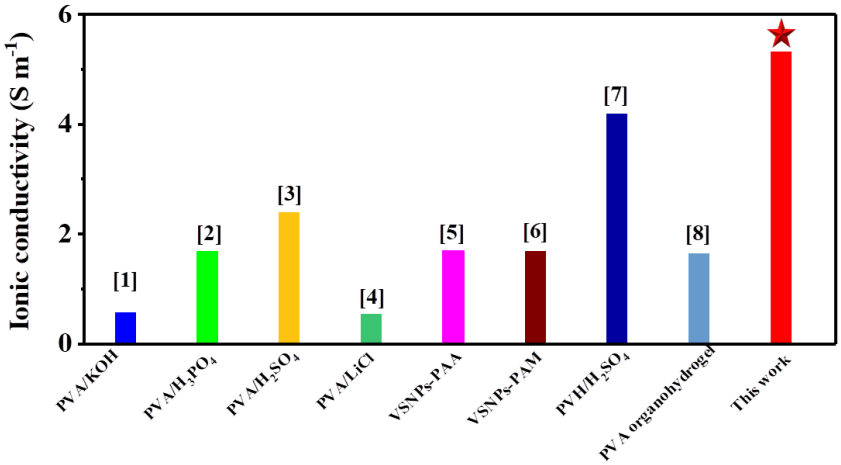

Figure S5. The ionic conductivity of AF-OHP and the previously reported polyelectrolytes at room temperature. [1] *Electrochim Acta* 2011, 56, 6881- 6886; [2] *Ionics* 2007, 13, 231-234; [3] *J. Power Sources* 2014, 266, 488-495; [4] *J. Mater. Chem. A* 2017, 5, 2759-2767; [5] *Nat. Commun.* 2015, 6, 10310; [6] *Angew. Chem., Int. Ed.* 2017, 56, 9141-9145; [7] *J. Mater. Chem. A* 2018, 6, 2500-2506; [8] *Adv. Energy Mater.* 2018, 8, 1801967.

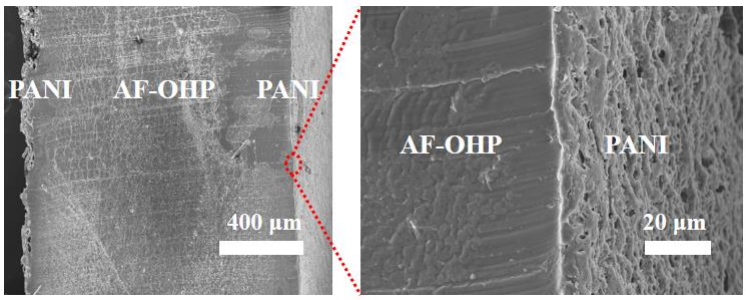

Figure S6. The cross-section SEM of oven-dried AF-SSC.

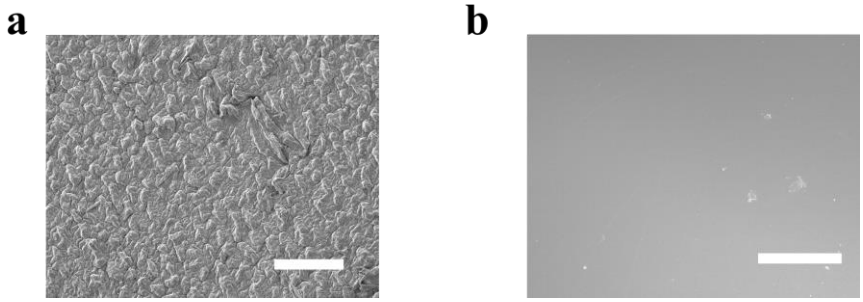

Figure S7. The surface morphology of a) oven-dried AF-SSC (Scale bar: 200 μm) and b) pure AF-OHP (Scale bar: 80 μm).

Figure S8. AF-SSC stably adhering to the surface of rubber gloves substrates without the extra adhesives even at the bending and stretching conditions.

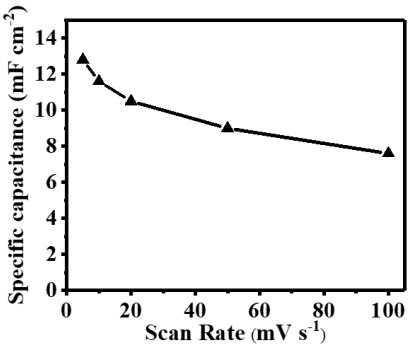

Figure S9. Specific capacitances of AF-SSC at the diverse scan rate.

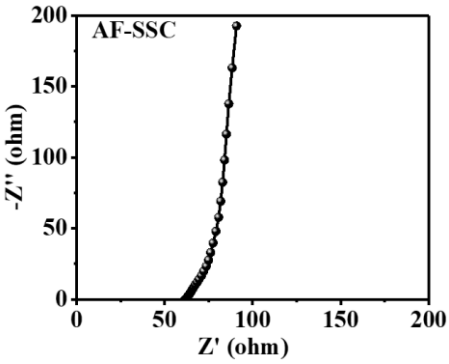

Figure S10. The electrochemical impedance spectroscopy of AF-SSC at the room

temperature.

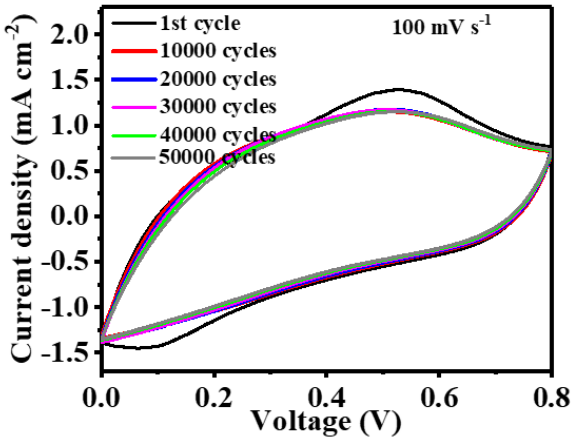

Figure S11. The CV curves after the different cycles at 100 mV s^{-1} of AF-SSC under the room temperature;

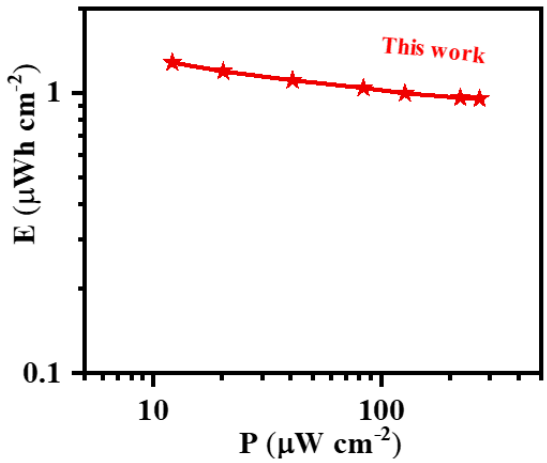

Figure S12. Ragone plots of the AF-SSC. The energy density of E(μWh cm^{-2}) and the power density P(μW cm^{-2}) were calculated by means of GCD curves following the equations: $E=1/2\ CU^2$, $P=E/\Delta t$, where C, U and Δt is specific capacitance, the operating voltage and the discharge time of SC, respectively.

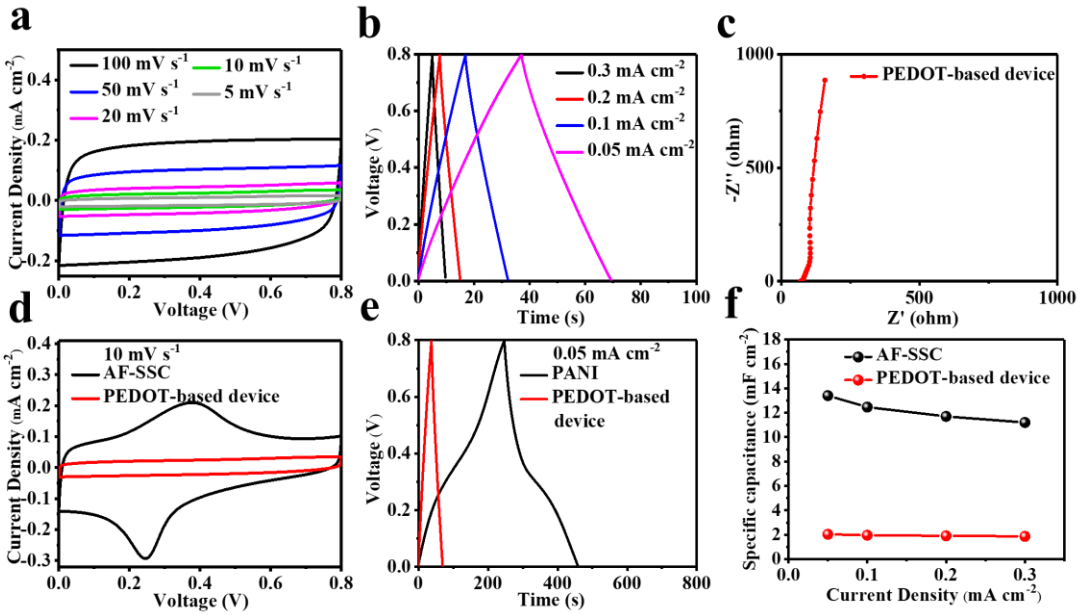

Figure S13. a) The CV curves, b) GCD curves and c) electrochemical impedance spectroscopy of the integrated SC based on PEDOT. d) The CV curves at 10 mV s^{-1}, e) GCD curves at 0.05 mA cm^{-2} and f) rate performance of the PEDOT-based device and AF-SSC. The CV curves of the PEDOT-based device present a quasi-rectangular shape and mirror-image symmetry at the scan rate of 5 to 100 mV s^{-1}, revealing its excellent capacitive behavior (Fig. S13a). As shown in Fig. 13b, the GCD curves at current densities ranging from 0.02 to 0.3 mA cm^{-2} exhibit typical triangular profiles, indicating highly reversible charge-discharge behavior of the device. The electrochemical impedance spectroscopy is performed to prove the small resistance and good capacitance behavior of the constructed SC device (Fig. 13c). However, compared with the PEDOT-based device, AF-SSC shows larger CV integral area, longer discharge time and higher specific capacity by reason of better pseudocapacitive characteristics of PANI (Fig. 13d-f).

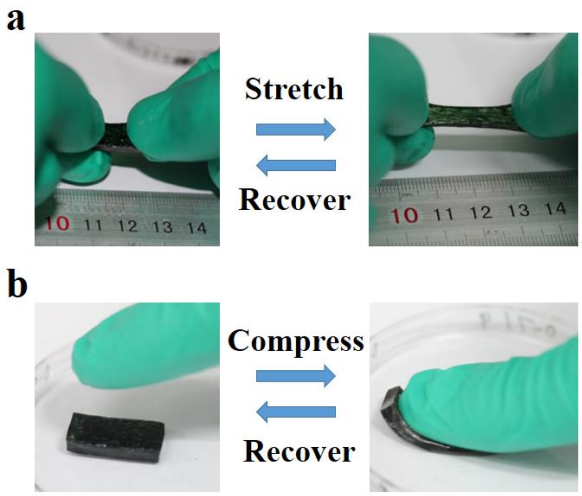

Figure S14. The high compression and excellent stretchability of AF-SSC after vacuum treatment for 20 h.

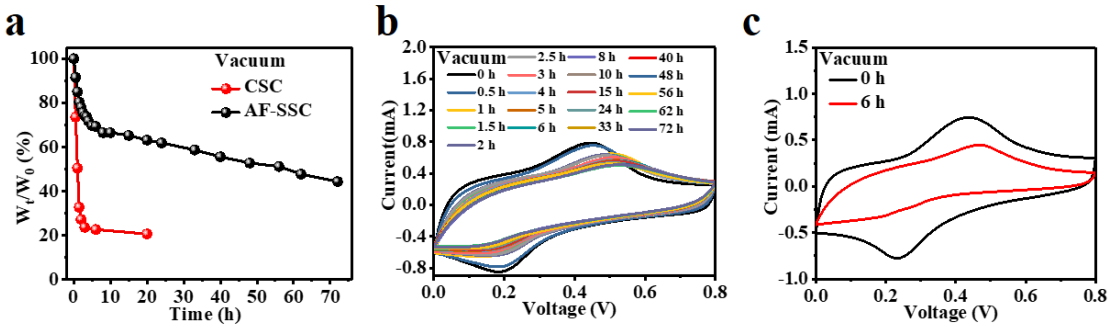

Figure S15. a) The mass retention of AF-SSC and CSC under vacuum environment for different time. The CV curves at the scan rate of 50 mV s^{-1} of b) AF-SSC and c) CSC under vacuum environment for different time.

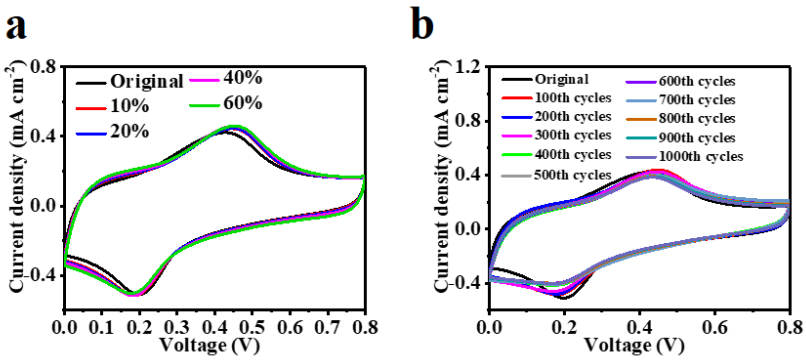

Figure S16. CV curves at the scan rate of 20 mV s^{-1} of AF-SSC a) under different compress ratio and b) after different compress/release cycles from the initial to 60%.

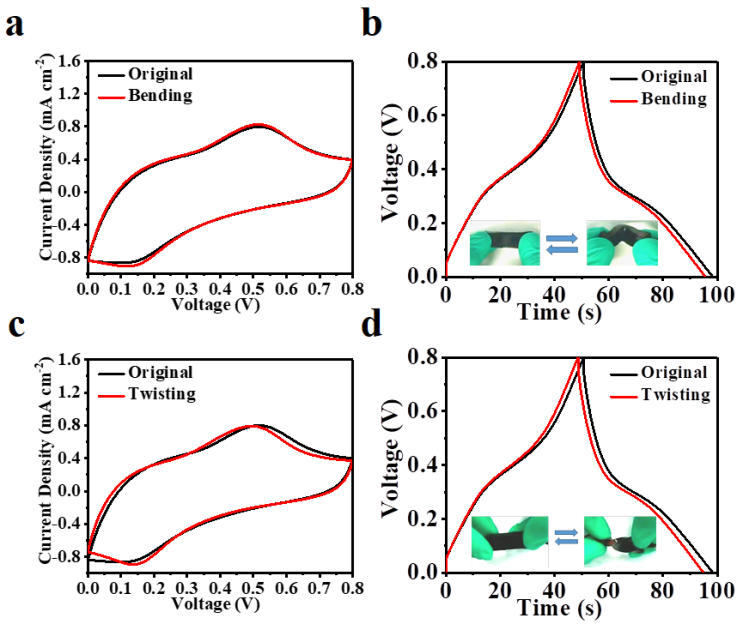

Figure S17. a) The CV curves at the scan rate of 20 mV s^{-1} and b) The GCD curves at the current density of 0.2 mA cm^{-2} of AF-SSC under bending. c) The CV curves at the scan rate of 20 mV s^{-1} and d) The GCD curves at the current density of 0.2 mA cm^{-2} of AF-SSC under twisting.

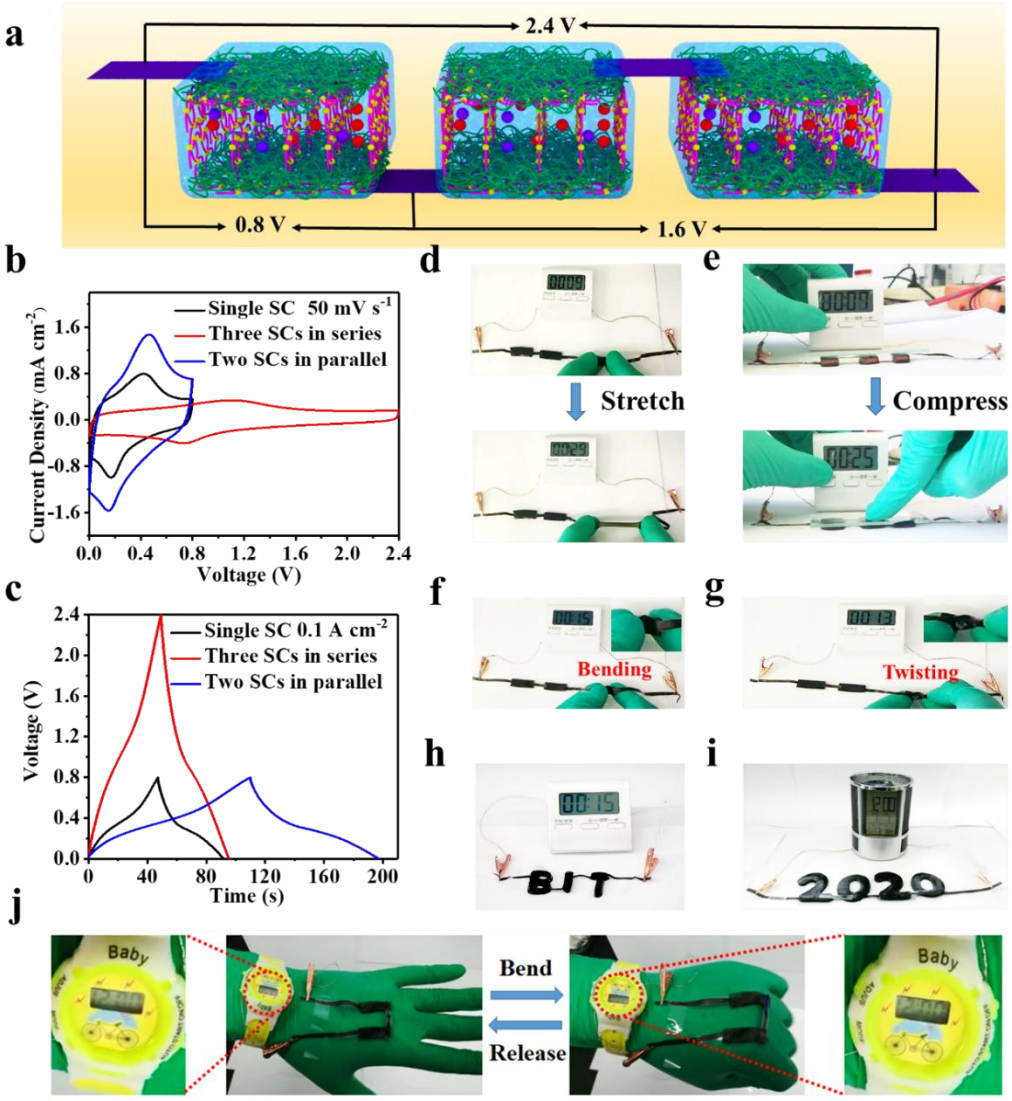

Figure S18. Performance of AF-SSCs with different patterns in series or parallel combinations under various deformation such as stretching, compressing, bending and twisting. a) Schematic illustration of three AF-SSCs connected in series. b) CV curves and c) GCD profiles of AF-SSCs connected in series or parallel. A commercialized timer powered by three AF-SSCs connected in series under d) stretching, e) compressing, f) bending and g) twisting. h) The timer driven by "BIT" patterned AF-SSCs assembled in series. i) A multifunctional pen holder displayer with music powered by "2020" patterned SCs assembled in series. j) An electronic watch powered by two

in-series AF-SSCs firmly adhered to the rubber gloves under bending.

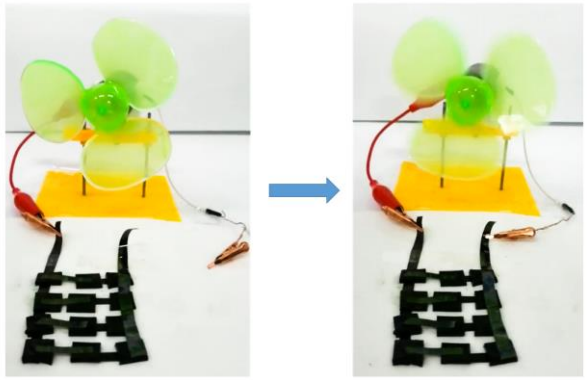

Figure S19. The electric fan powered by AF-SSCs in series and parallel.

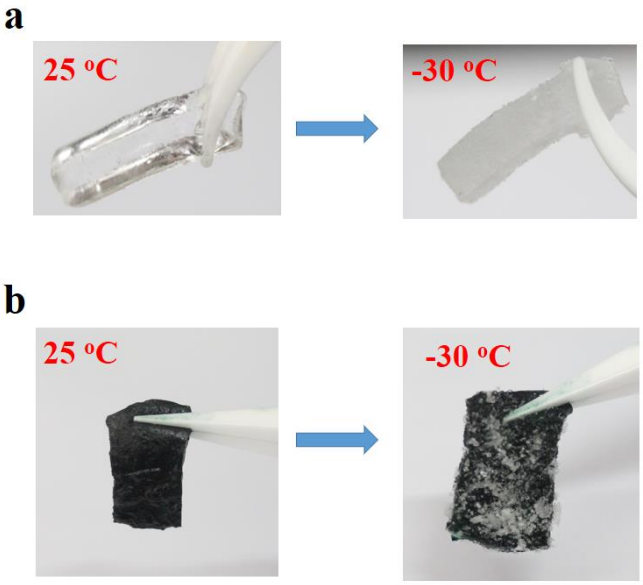

Figure S20. The optical photograph of a) the frozen C-PAM hydrogel polyelectrolyte and b) the frozen CSC at -30 °C.

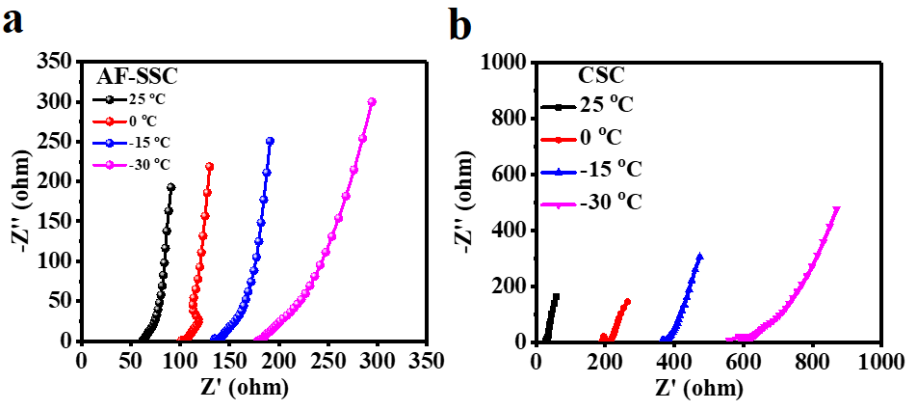

Figure S21. The electrochemical impedance spectroscopy under different temperature

of a) AF-SSC and b) CSC.

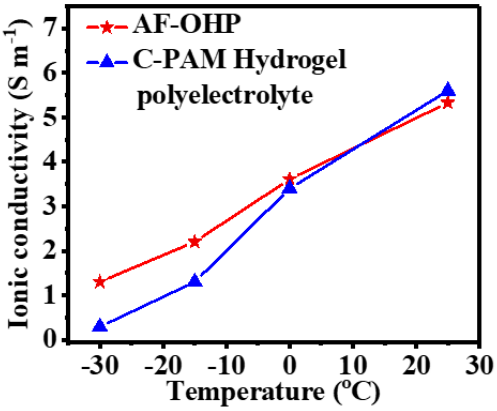

Figure S22. The ionic conductivity of AF-OHP and C-PAM polyelectrolyte under different temperature.

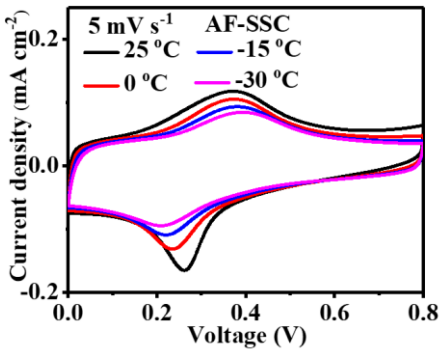

Figure S23. CV curves of AF-SSC under different temperature.

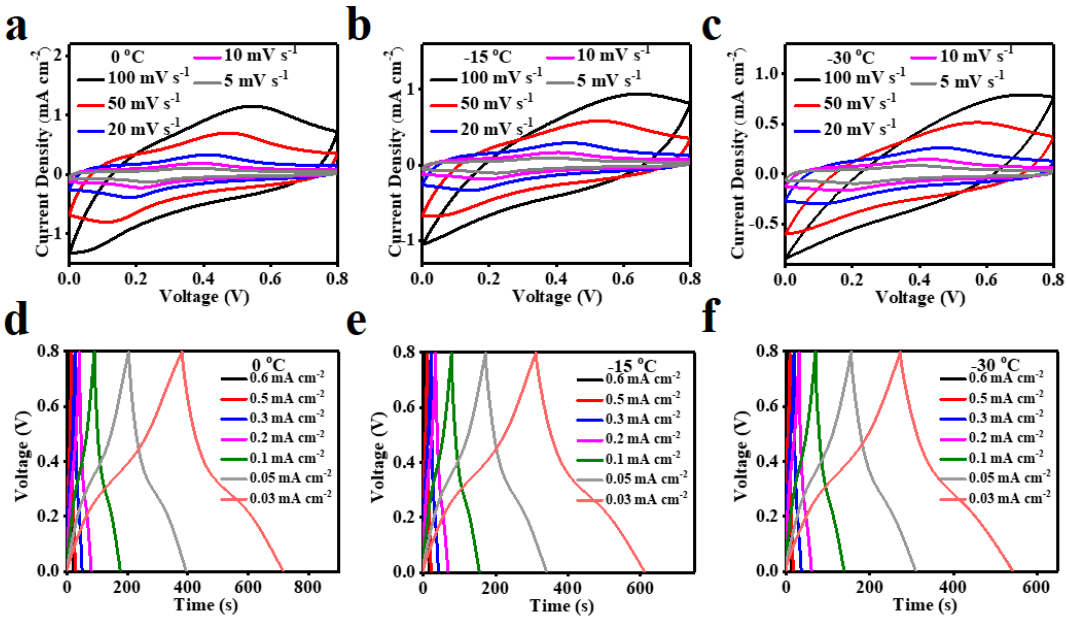

Figure S24. The CV curves at the different scan rate a) under 0 °C, b) under -15 °C, and c) under -30 °C. The GCD curves at the different current density d) under 0 °C, e) under -15 °C and f) under -30 °C.

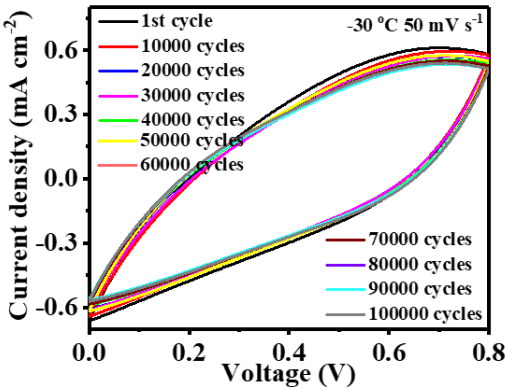

Figure S25. The CV curves after the different cycles at 50 mV s^{-1} of AF-SSC under -30 °C.

Table S1. The calculated interaction energy of bonding pairs in EG-W, W-W, EG-EG.

Model	Interaction Energy (eV)	Interaction Energy (Kcal/mol)

W-W	-0.16	-3.74
EG-EG	-0.24	-5.57
W-EG	-0.21	-4.86

Table S2. The calculated interaction energy of bonding pairs in PAM-W, PAM-EG, PAM-W-EG

Model	Interaction Energy (eV)	Interaction Energy (Kcal/mol)
PAM-W	-0.42	-9.68
PAM-EG	-0.21	-4.99
PAM-W-EG	-1	-23.15

Table S3 Multifunctional comparison of AF-SSC and the previously reported SSCs

	Temperature tolerance	Stretch Ratio	Substrate/ Geometric design	Cycles life, capacitance retention	Reversible compression ratio	Process ability	Anti-drying ability
This work	**-30 ºC to 25 ºC**	**200% at 25 and -30 ºC**	**No Need**	**100000 cycles at -30 oC , 91.7%; 50000 cycles at 25 ºC, 84.7%**	**60%**	**Yes**	**Yes**
[1] Adv Energy Mater 2016, 6, 1600050	Room Temperature	50%	Polydimethylsiloxane (PDMS)	10000 cycles, 96%	No	No	No
[2] Adv Energy Mater 2017, 7, 1600976	Room Temperature	20%	Helical structure	5000 cycles, 80%	No	No	No
[3] Adv Funct Mater. 2017, 27, 1704353	Room Temperature	30%	PDMS	2000 cycles, 100%	No	No	No
[4] Angew Chem Int Ed 2013, 52,	Room Temperature	100%	Elastic fiber	1000 cycles, 100%	No	No	No

13453							
[5] Adv Mater 2018, 30, 1800124	Room Temperature	40%	Spring structure	17000 cycles, 86%	No	No	No
[6] Nano Energy 2017, 39, 219	Room Temperature	100%	Elastic fiber	5000 cycles, 90.7%	No	No	No
[7] Nano Energy 2016, 27, 230	Room Temperature	130%	Urethane plastic fiber	None	No	No	No
[8] ACS Nano 2017, 11, 9490	Room Temperature	100%	Knitting structure	6000 cycles, 78%	No	No	No
[9] ACS Nano 2017, 11, 2066	Room Temperature	100%	Spring structure	None	No	No	No
[10] ACS Nano 2019, 13, 10469	Room Temperature	50%	Knitted fabric	10000 cycles, 76%	No	No	No
[11] Adv Mater 2009, 21, 4793	Room Temperature	30%	PDMS	1000 cycles, 100%	No	No	No
[12] Advanced Materials, 2014, 26, 4444.	Room Temperature	100%	PDMS	2000 cycles, 98%	No	No	No
[13] Nature Commun, 2016, 7:13811	Room Temperature	30%	Coiled structure	1000 cycles, 98.4%	No	No	No
[14] Adv. Funct. Mater. 2015, 25, 4601	Room Temperature	30%	PVA film	1000 cycles, 97%	No	No	No
[15] Nat Commun 2020, 11, 62	Room Temperature	200%	Polyvinyl alcohol (PVA)	6000 cycles, 80%	50%	No	No
[16] Nat Commun, 2019, 10, 536	Room Temperature	1000%	Wrinkle	10000 cycles, ~96%	No	No	No
[17] Nat. Commun. 6, 10310 (2015).	Room Temperature	600%	Wrinkle	None	80%	No	No
[18] Adv Mater 2018, 30, 1704531	Room Temperature	500%	Geometric design	10000 cycles, 95%	No	Yes	No
[19] Adv Mater. 2019, 31, 1900573	Room Temperature	800%	Gold nanoparticle/CNT/poly(acrylamide)	10000 cycles, 93%	No	No	No
[20] Nano Energy 2015, 11, 518	Room Temperature	20%	Steel mesh	10000 cycles, 98%	No	No	No
[21] Adv. Energy Mater. 2019, 9, 1900618	Room Temperature	800%	Elastomer substrates	10000 cycles, 91.6%	No	No	No
[22] Adv. Energy Mater. 2017, 7, 1601814	Room Temperature	400%	Polyurethane	10000 cycles, 92%	No	No	No

[23] ACS Nano 2020, 14, 3576	Room Temperature	300%	Elastomer substrates	10000 cycles, 85%	No	No	No
[24] Angew. Chem. Int. Ed.2016, 55, 9191-9195	Room Temperature	240%	PDMS	10000 cycles, 98%	No	No	No
[25] ACS Nano 2016, 10, 5204-5211.	Room Temperature	200%	Silicon rubber	None	No	No	No
[26] Energy Storage Materials, 2020, 25, 124.	Room Temperature	200%	Elastic fiber	None	No	No	No
[27] ACS Nano, 2015, 9, 6088.	Room Temperature	100%	Elastic fiber	10000 cycles, 99%	No	No	No
[28] Adv. Mater. 2013, 25, 2326	Room Temperature	200%	Spring structure	None	No	No	No
[29] Adv. Energy Mater. 2016, 7, 1602021	Room Temperature	800%	Rubber fiber	1000 cycles, 100%	No	No	No
[30] Nano Lett. 2016, 16, 7677	Room Temperature	200%	Elastic fiber	1000 cycles, 94.8%	No	No	No
[31] Angew. Chem., Int. Ed. 2017, 56, 9141	Room Temperature	1000%	Wrinkle	None	50%	No	No
[32] Angew Chem Int Ed 2019, 58, 15707-15711	Room Temperature	200%	Wrinkle	4000 cycles, 95.2%	No	No	No